Einstein@Home DISCOVERY OF A PALFA MILLISECOND PULSAR IN AN ECCENTRIC BINARY ORBIT

B. Knispel[1,2,†], A. G. Lyne[3], B. W. Stappers[3], P. C. C. Freire[4], P. Lazarus[4], B. Allen[2,5,1], C. Aulbert[2], O. Bock[2],
S. Bogdanov[6], A. Brazier[7,8], F. Camilo[6], F. Cardoso[9], S. Chatterjee[7], J. M. Cordes[7], F. Crawford[10], J. S. Deneva[11],
H.-B. Eggenstein[2], H. Fehrmann[2], R. Ferdman[12], J. W. T. Hessels[13,14], F. A. Jenet[15], C. Karako-Argaman[12], V. M. Kaspi[12],
J. van Leeuwen[13,14], D. R. Lorimer[9], R. Lynch[12], B. Machenschalk[2], E. Madsen[12], M. A. McLaughlin[9], C. Patel[12],
S. M. Ransom[16], P. Scholz[12], X. Siemens[5], L. G. Spitler[4], I. H. Stairs[17], K. Stovall[18], J. K. Swiggum[9], A. Venkataraman[19],
R. S. Wharton[7], W. W. Zhu[4,17]
To appear in ApJ

ABSTRACT

We report the discovery of the millisecond pulsar (MSP) PSR J1950+2414 ($P = 4.3$ ms) in a binary system
with an eccentric ($e = 0.08$) 22-day orbit in Pulsar ALFA survey observations with the Arecibo telescope. Its
companion star has a median mass of $0.3 \, M_\odot$ and is most likely a white dwarf. Fully recycled MSPs like this
one are thought to be old neutron stars spun-up by mass transfer from a companion star. This process should
circularize the orbit, as is observed for the vast majority of binary MSPs, which predominantly have orbital
eccentricities $e < 0.001$. However, four recently discovered binary MSPs have orbits with $0.027 < e < 0.44$;
PSR J1950+2414 is the fifth such system to be discovered. The upper limits for its intrinsic spin period
derivative and inferred surface magnetic field strength are comparable to those of the general MSP population.
The large eccentricities are incompatible with the predictions of the standard recycling scenario: something
unusual happened during their evolution. Proposed scenarios are a) initial evolution of the pulsar in a triple
system which became dynamically unstable, b) origin in an exchange encounter in an environment with high
stellar density, c) rotationally delayed accretion-induced collapse of a super-Chandrasekhar white dwarf, and
d) dynamical interaction of the binary with a circumbinary disk. We compare the properties of all five known
eccentric MSPs with the predictions of these formation channels. Future measurements of the masses and proper
motion might allow us to firmly exclude some of the proposed formation scenarios.

Subject headings: methods: data analysis, stars: neutron, pulsars: general, pulsars: individual (J1950+2414)

1. INTRODUCTION

† Email: benjamin.knispel@aei.mpg.de
[1] Leibniz Universität, Hannover, D-30167 Hannover, Germany
[2] Max-Planck-Institut für Gravitationsphysik, Callinstr. 38, D-30167
Hannover, Germany
[3] Jodrell Bank Centre for Astrophysics, School of Physics and Astronomy, University of Manchester, Manchester, M13 9PL, UK
[4] Max-Planck-Institut für Radioastronomie, Auf dem Hügel 69, 53121
Bonn, Germany
[5] Physics Department, University of Wisconsin – Milwaukee, Milwaukee
WI 53211, USA
[6] Columbia Astrophysics Laboratory, Columbia University, New York,
NY 10027, USA
[7] Department of Astronomy and Center for Radiophysics and Space Research, Cornell University, Ithaca, NY 14853, USA
[8] Cornell Center for Advanced Computing, Rhodes Hall, Cornell, University, Ithaca, NY 14853, USA
[9] Department of Physics and Astronomy, West Virginia University, Morgantown, WV 26506, USA
[10] Department of Physics and Astronomy, Franklin and Marshall College,
Lancaster, PA 17604-3003, USA
[11] National Academies of Science, resident at the Naval Research Laboratory, Washington, DC 20375, USA
[12] Department of Physics, McGill University, Montreal, QC H3A 2T8,
Canada
[13] ASTRON, Netherlands Institute for Radio Astronomy, Postbus 2, 7990
AA, Dwingeloo, The Netherlands
[14] Anton Pannekoek Institute for Astronomy, University of Amsterdam,
Science Park 904, 1098 XH Amsterdam, The Netherlands
[15] Center for Gravitational Wave Astronomy, University of Texas at
Brownsville, TX 78520, USA
[16] NRAO, Charlottesville, VA 22903, USA
[17] Department of Physics and Astronomy, University of British Columbia,
6224 Agricultural Road Vancouver, BC V6T 1Z1, Canada
[18] Department of Physics and Astronomy, University of New Mexico,
NM, 87131, USA
[19] Arecibo Observatory, HC3 Box 53995, Arecibo, PR 00612, USA

Millisecond pulsars (MSPs; Backer et al. 1982) are thought
to be old neutron stars (NS) spun up by mass accretion and
transfer of angular momentum from a companion star (Radhakrishnan & Srinivasan 1982; Alpar et al. 1982). The spin
frequencies of these so-called "recycled" pulsars can range up
to 716 Hz (Hessels et al. 2006; ATNF pulsar catalog, Manchester et al. 2005). The different evolutionary phases of these
pulsars in binary systems and also the transitions between
these phases have been recently observed in much more detail, though several major puzzles still remain. The binary
system starts off as a low-mass X-ray binary in which a NS
accretes matter from a companion star (Smarr & Blandford
1976; Bildsten et al. 1997). The main emission from these system is X-rays from the hot accretion disk. These system can
transition into an accreting X-ray MSP in a binary (Wijnands
& van der Klis 1998), in which matter is funnelled onto the
neutron star's surface and significant X-ray emission modulated by the NS spin is detected. After the accretion dies off,
the NS can become "visible" as a radio MSP, powered by the
rotation of the neutron star's magnetic field (Tauris & Savonije
1999; Stairs 2004). In some cases, these systems are seen to
switch on roughly year-long timescales between states as an
LMXB and a radio MSP. For example, Archibald et al. (2009)
showed that the radio MSP PSR J1023+0038 has turned on after a recent ($\sim$10 yrs) LMXB phase; more recently this system
changed back into an LMXB (Archibald et al. 2014; Patruno
et al. 2014; Stappers et al. 2014). Similarly, LMXB/radio MSP
state transitions have been shown for PSRs J1824−2452 and
J1227−4853 (Papitto et al. 2013; Bassa et al. 2014; Roy et al.
2015). Together, these observations nicely demonstrate the
basic recycling scenario; however, they have also raised new
puzzles and shown that the details of the process are quite

complex. It is also possible that these three aforementioned transitional MSP systems, all "redback" MSPs (Roberts 2013), are not representative of the evolution of all types of MSPs and that these systems might not lead to recycled pulsars at all (Chen et al. 2013). As such, much remains to be understood in the formation of radio MSPs.

The recycling pathway results in highly circular orbits of the binary system through tidal forces acting during the $10^8 - 10^9$ year long accretion phase (Phinney & Kulkarni 1994). Until 2008, this seemed true of all fully recycled MSPs. All binary pulsars with $\nu \geq 50\,\mathrm{Hz}$ and $\dot{\nu} \leq 10^{-14}\,\mathrm{Hz\,s^{-1}}$ outside of globular clusters had orbital eccentricities between $e = 10^{-7}$ and $e = 10^{-3}$ (Manchester et al. 2005).These eccentricity limits do not apply to MSPs in globular clusters because their high stellar densities and resultant close stellar encounters can significantly increase the orbital eccentricity of a binary MSP after the end of the accretion phase (Rasio & Heggie 1995; Heggie & Rasio 1996) or even in some cases lead to exchange encounters. Indeed, several highly eccentric binary MSPs have been found in the Galactic globular cluster system (e.g., Ransom et al. (2005); see also the online catalog of globular cluster pulsars at http://www.naic.edu/~pfreire/GCpsr.html).

In 2008, the situation changed with the discovery of PSR J1903+0327. This fast-spinning MSP ($P = 2.15\,\mathrm{ms}$) in an eccentric orbit ($e = 0.44$) with a $\sim 1\,M_\odot$ main-sequence star (Champion et al. 2008) cannot have formed through the "normal" binary evolution described above. Rather, it is believed to have originated from a hierarchical triple that became dynamically unstable (Freire et al. 2011; Portegies Zwart et al. 2011; Pijloo et al. 2012).

Soon afterwards, Bailes (2010) reported an "anomalous" orbital eccentricity of 0.027 for PSR J1618−3921 (Bailes; private communication), a MSP first reported in Edwards & Bailes (2001). More recently, Deneva et al. (2013) and Barr et al. (2013) reported the discovery of two more unusual binary MSP systems PSR J2234+06 ($e = 0.13$) and PSR J1946+3417 ($e = 0.14$). These three systems are fully recycled with spin periods between 3 and 12 ms, orbital periods P_{orb} from 22 to 32 days and median companion masses $M_2 \approx 0.25\,M_\odot$; i.e., apart from the large orbital eccentricity all parameters are compatible with the canonical recycling formation channel leading to a MSP with a white dwarf (WD) companion as described above.

These unusual orbital eccentricities require a non-standard formation channel. Like PSR J1903+0327, they *could* have formed in a triple system which later became unstable and ejected the outer (tertiary) companion. In fact, fully recycled MSPs can form in stable triple systems, as shown by the discovery of PSR J0337+1715, the first MSP in a stellar triple system with two white dwarf companions (Ransom et al. 2014; Tauris & van den Heuvel 2014).

However, the chaotic disruption of a triple system would most likely not lead to the formation of MSPs with very similar orbital and spin characteristics as discussed above. These similarities suggest instead a more orderly mechanism with a more predictable outcome.

A possibility for such a mechanism was proposed by Freire & Tauris (2014). They suggest these systems formed through an accretion-induced collapse (AIC) of a super-Chandrasekhar mass oxygen-neon-magnesium white dwarf in a close binary. This star initially avoids AIC due to its rapid rotation. Only after the end of the accretion episode, and after the WD loses sufficient spin angular momentum, does it undergo AIC to

directly produce an MSP in an eccentric orbit. A second possibility was suggested by Antoniadis (2014): here the MSPs form through the usual channel, but the orbital eccentricity arises from the dynamical interaction with a circumbinary disk. This disk may form from donor material ejected during hydrogen-shell flash episodes. Antoniadis (2014) shows that even a short-lived disk can produce eccentricities as large as $e = 0.15$.

Here we present the discovery and initial timing of the binary MSP PSR J1950+2414 in Pulsar ALFA (PALFA) survey data obtained at 1.4 GHz with the Arecibo telescope. This is the fifth eccentric MSP in the Galactic field to be discovered; its orbital and spin parameters are similar to those of PSR J2234+06 and PSR J1946+3417.

First, we will briefly describe the PALFA survey, the *Einstein@Home* project and its analysis of PALFA survey data, and the discovery of PSR J1950+2414. We then describe the timing observations, data reduction, and timing solution, followed by a discussion of PSR J1950+2414. We discuss our discovery in the context of different possible formation channels for MSPs in eccentric binaries. We conclude with an overview of future studies of this pulsar system and how they might allow us to exclude some of the possible formation channels.

1.1. *The PALFA Survey*

The PALFA Survey (Cordes et al. 2006) was proposed and is managed by the PALFA Consortium. It consists of about 40 researchers (including students) at about ten institutions worldwide[21].

At Arecibo Observatory, the PALFA Consortium uses the Arecibo L-band Feed Array (ALFA[22]). The output of the seven ALFA beams is fed into the Mock spectrometers[23]. The observing band of 322.6 MHz is split into two overlapping bands with bandwidths of 172.0625 MHz each. The two sub-bands are centred at 1300.1680 MHz and 1450.1680 MHz, respectively. A total of 960 frequency channels is used, generated by polyphase filterbanks to enable the correction of radio pulse dispersion in the interstellar medium. Spectra are sampled every 65.4762 μs.

The PALFA survey setup (high observation frequency, large number of filterbank channels, fast-sampling spectrometers) is chosen to maximize the chances of discovering MSPs at large distances within the Galactic plane, where previous surveys have had little to no sensitivity to MSPs. At the same time, the detection of these objects has been difficult because of their high values of dispersion measure (DM), which induce high dispersive smearing per channel. The narrow channels used in the PALFA survey address this issue. Finding many MSPs is the highest priority in this survey because of their wide range of astrophysical applications: testing Einstein's theory of general relativity and alternative theories of gravity (Antoniadis et al. 2013), measuring NS masses (Demorest et al. 2010), which can strongly constrain the equation of state of dense matter, finding suitable sources for pulsar timing arrays (Hobbs et al. 2010), which will be used for detection of very low-frequency gravitational waves, improved estimates of the Galactic MSP population (Swiggum et al. 2014), and

---

[21] http://www2.naic.edu/alfa/pulsar/

[22] http://www.naic.edu/alfa/

[23] Details of the Mock spectrometers may be found on the following NAIC web page: http://www.naic.edu/~phil/hardware/pdev/pdev.html

– in the case of PSR J1950+2414 and similar systems – a better understanding of stellar and NS formation and evolution. PALFA discoveries are proof of the power of the survey to discover MSPs at high DMs (Champion et al. 2008; Knispel et al. 2010, 2011; Crawford et al. 2012; Deneva et al. 2012).

Since its first observations in 2004, the PALFA Consortium has been surveying the part of the sky close to the Galactic plane ($|b| \leq 5°$) that is visible to Arecibo Observatory, i.e., declinations $0° \leq \delta \leq 37°$. The complete survey of this sky area will require about 330,000 separate Arecibo beams (equivalent to $\sim 47,000$ pointings of the seven-beam ALFA receiver).

Data from the PALFA survey are analyzed by the *Einstein@Home* pipeline briefly described below and also by an independent pipeline operating on a supercomputer at McGill University using the `PRESTO` software package[24] (Lazarus et al., in prep.).

1.2. *Einstein@Home*

Einstein@Home[25] is a distributed volunteer computing project (Anderson et al. 2006). Members of the public donate otherwise unused compute cycles on their home and/or office PCs, and Android devices to the project to enable blind searches for unknown NS.

Einstein@Home is one of the largest distributed computing projects. In the last ten years since its launch, more than 390,000 volunteers have contributed to the project. On average, about 46,000 different volunteers donate computing time each week on roughly 105,000 different hosts[26]. The sustained computing power provided by these volunteers is currently of order $1.75\,\mathrm{PFlop\,s^{-1}}$, which is $\sim 5\%$ the computing power of the world's fastest supercomputer

Einstein@Home analyzes data from the LIGO gravitational-wave detectors, the *Fermi Gamma-ray Space Telescope*, and large radio telescopes such as the Arecibo Observatory and the Parkes Radio Telescope. Observational data are stored and prepared for *Einstein@Home* processing on the Atlas computer cluster at the Albert Einstein Institute in Hannover, Germany (Aulbert & Fehrmann 2009). Volunteers' computers download the data along with scientific software from dedicated servers in Hannover and Milwaukee, and run it automatically. The central coordination and management of the computing is handled by the Berkeley Open Infrastructure for Network Computing (BOINC; Anderson et al. (2006)).

The *Einstein@Home* PALFA analysis pipeline consists of three main steps. 1) Observational data are de-dispersed at $\sim 4,000$ trial values to mitigate the radio pulse dispersion from the signal passing through the interstellar medium. Strong burst-like RFI is masked and periodic RFI is identified and replaced by random noise. Step 2) is done on the computers of the general public, attached to the project: each resulting de-dispersed time series is analyzed for periodic radio pulsar signals using Fourier methods. The *Einstein@Home* pipeline searches for radio pulsars in compact binary systems with orbital periods as short as 11 min. The required orbital demodulation to remove the Doppler effect from binary motion is done in the time domain. The demodulation is repeated for $\sim 7,000$ different orbital configurations to cover a wide range of possible physical orbital parameters. For each of these, the

Fourier analysis is repeated after the time-domain demodulation. The 100 statistically most significant candidates from each de-dispersed time series are stored and sent back to the project servers in Hannover. 3) The resulting $\sim 400,000$ candidates for each beam are sifted and remaining candidates folded using the raw data and graded by machine learning methods (Zhu et al. 2014). Per-beam overview plots are also visually inspected to identify (of order a few) promising candidates in each beam.

A full description of the *Einstein@Home* radio pulsar search pipeline employed to discover PSR J1950+2414 is beyond the scope of this publication and is available in Allen et al. (2013). The sifting techniques used to reduce the number of relevant candidates are described in Knispel (2011); Knispel et al. (2013)

To date, the project has discovered 51 neutron stars through their radio emission. As part of the PALFA collaboration, *Einstein@Home* has discovered a total of 27 radio pulsars[27], including the fastest spinning disrupted recycled pulsar (i.e., a pulsar ejected from a binary system due to the companion star's supernova explosion; Knispel et al. 2010), and a relativistic intermediate-mass binary pulsar (Knispel et al. 2011; Lazarus et al. 2014). The *Einstein@Home* search for radio pulsars in archival data from the Parkes Radio Telescope has found 24 pulsars missed by several previous re-analyses of this data set (Knispel et al. 2013).

Einstein@Home has to date also discovered four gamma-ray pulsars in *Fermi* data (Pletsch et al. 2013). These ongoing searches use highly efficient data analysis methods initially conceived for gravitational-wave data analysis (Pletsch & Allen 2009; Pletsch 2010, 2011; Pletsch et al. 2012).

The detection of continuous gravitational waves from rotating neutron stars in data from ground-based interferometric detectors is the main, long-term goal of *Einstein@Home*. The project has provided the most stringent upper limits for gravitational waves from rapidly rotating neutron stars in blind searches to date (Abbott et al. 2009a,b; Aasi et al. 2013).

1.3. *Discovery of PSR J1950+2414*

PSR J1950+2414 was discovered by the *Einstein@Home* PALFA pipeline on 2011 October 4 with a statistical significance $\mathcal{S} = 120.8$ (negative decadic logarithm of the false-alarm probability in Gaussian noise) in a PALFA survey observation from 2009 April 4. The pulsar was found at a spin period of $4.3\,\mathrm{ms}$ and a DM of $142\,\mathrm{pc\,cm^{-3}}$. The signal's celestial nature was confirmed the same day with a second observation by the Arecibo telescope.

2. OBSERVATIONS AND DATA ANALYSIS

2.1. *Observations*

Following its discovery, PSR J1950+2414 was observed during the PALFA survey observing sessions and with dedicated observations by the 76-m Lovell telescope at Jodrell Bank.

The observations with the Arecibo telescope employed the usual PALFA survey set up as described in Section 1.1, using only the central beam of ALFA. The durations were between 4.5 mins and 15 mins. In total 24 PALFA survey observations

---

[24] https://github.com/scottransom/presto
[25] http://einsteinathome.org
[26] http://einsteinathome.org/server_status.html as of early April 2015

[27] All discoveries are available online at http://einsteinathome.org/radiopulsar/html/rediscovery_page/rediscoveries.html and http://einsteinathome.org/radiopulsar/html/BRP4_discoveries/

of PSR J1950+2414 were carried out from 2011 October 5 until 2012 May 5.

Between 2012 September 21 and 2012 December 31, nine dedicated timing observations of PSR J1950+2414 were carried out as part of a PALFA millisecond pulsar timing campaign. Observations used the L-wide receiver and the Puerto-Rican Ultimate Pulsar Processing Instrument (PUPPI) backend. A frequency band of 800 MHz in 2048 channels, centered on a frequency of 1380 MHz was observed in all sessions. The usable bandwidth is limited by the L-wide receiver which delivers an observation bandwidth of 700 MHz from 1.1 GHz to 1.8 GHz. Observation times were 10 mins or 15 mins with a sampling time of 40.96 μs.

The observations with the 76-m Lovell telescope used a cryogenically-cooled dual-polarization receiver at a central frequency of about 1520 MHz. A 512-MHz band was sampled at 8-bits resolution and processed using a digital filter bank into 2048 0.25-MHz frequency channels. After radio frequency interference excision, approximately 384 MHz of usable bandwidth remained. The data were folded into 1024 pulse phase bins and were de-dispersed, generating an average profile for each 10-second sub-integration. Observations of mostly 30 mins duration were made approximately every 10 days and the data set includes 61 TOAs from the MJD period 55851 to 56272.

2.2. *Data reduction*

Observational data were processed offline for radio frequency interference (RFI) mitigation, and to obtain times-of-arrival (TOAs).

The separate sub-band data files obtained with the PALFA Mock spectrometers were merged into one file in PSRFITS format for each observation. PUPPI data were written in separate PSRFITS files, each covering adjacent observation time stretches.

For RFI mitigation, the `rfifind` program from the `PRESTO` pulsar processing suite was used to generate an RFI mask for each observation.

Each observation was folded at the appropriate dispersion measure and topocentric spin period with the `prepfold` program from `PRESTO`. Folded data files were used to create summed pulse profiles from all ALFA/Mock spectrometer observations and all L-wide/PUPPI observations, respectively. Fig. 1 shows these pulse profiles, averaged over 25 observations with the Mock spectrometers and over ten observations with the PUPPI backend, respectively. The full width at half maximum duty cycle is 8%. This corresponds to a width of the pulse of $w_{50} = 0.34$ ms. The dispersive delay across a single frequency channel is 0.18 ms for the given DM, frequency resolution and central frequency. An exponential scattering tail is apparent in the folded pulse profile. Centered on a rotational phase of 0.65 a small additional pulse component appears in both the ALFA/Mock and L-wide/PUPPI observations.

We calibrate the profile using the radiometer equation (e.g., Lorimer & Kramer 2012)

$$\sigma = \frac{S_{\text{sys}}}{\sqrt{2\Delta_f T_{\text{obs}}/N}} \qquad (1)$$

to predict the observing system's noise level σ. We assume a system equivalent flux density $S_{\text{sys}} = 2.4$ Jy for the L-wide receiver [28]. The combined observation bandwidth of L-wide
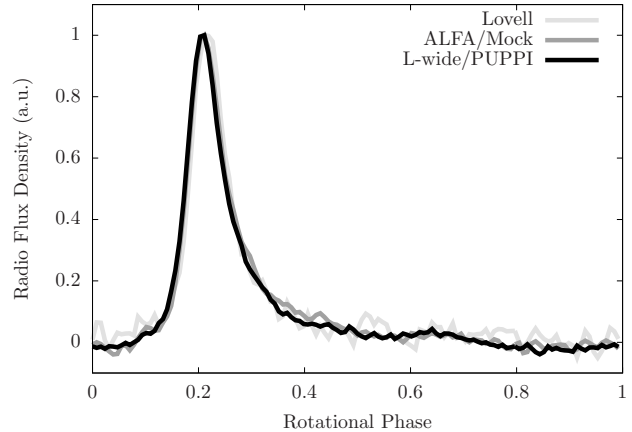
Figure 1. The averaged radio flux density pulse profiles from the data collected with Arecibo Observatory using the Mock spectrometers and the ALFA receiver (dark-grey line) and with the PUPPI backend and the L-wide receiver (black line), respectively. The averaged radio flux density pulse profile from observations at the Lovell Telescope in Jodrell Bank is shown (light-grey line). The spin period of the pulsar is 4.3 ms. These profiles were used to obtain the TOAs. All pulse profiles have been normalized and aligned at their maximum. The period-averaged flux density at 1.4 GHz is $S_{1400} = 119 \pm 13 \, \mu$Jy.

with the PUPPI backend is $\Delta_f = 700$ MHz. We used a pulse profile summed from nine individual observations, six of which with 9.8 mins duration and three with 14.9 mins duration. The summed pulse profile was folded into $N = 128$ bins; then the expected off-pulse noise standard deviation used for calibration is 9.2 μJy. Scaling the off-pulse noise level of the observations (between pulse phases 0.73 and 1.07 in Fig. 1), the resulting estimated period-averaged flux density of the pulsar at 1.4 GHz is $S_{1400} = 119 \pm 13 \, \mu$Jy.

The `get_TOAs.py` routine from `PRESTO` was used to extract TOAs by employing the sums of pulse profiles as templates. A single TOA was extracted for each ALFA/Mock spectrometer and L-wide/PUPPI observation, respectively. A total of 33 TOAs was extracted from the data obtained with the Arecibo telescope, 24 of which with the Mock spectrometer, the remaining 9 with the PUPPI backend.

The PSRCHIVE[29] package by Hotan et al. (2004) was used for the data inspection, interference removal and arrival time determination in the Lovell Telescope data. A single TOA was generated for each of the observations using a high signal-to-noise template formed from the observations.

The timing analysis used the `TEMPO2` software (Hobbs et al. 2006). Our timing solution uses the BT orbital model (Blandford & Teukolsky 1976; Edwards et al. 2006). The coherent solution fits 94 TOAs obtained between MJDs 55839 and 56293, covering a baseline of 454 days. As visible in Fig. 2, the timing model accurately predicts TOAs. There are no clear trends in the TOA residuals as a function of time, nor as a function of binary orbital phase. Constant time offsets between the three TOA data sets have been fitted with `TEMPO2`.

The weighted RMS of the timing residuals is 4.7 μs when including TOAs from both observatories with all receivers and backends. The most precise TOAs are obtained with the PUPPI backend and the L-wide receiver at Arecibo. For an observation time of 15 mins, the TOAs have an average precision of 1.3 μs. This makes PSR J1950+2414 an interesting pulsar to be used in Pulsar Timing Arrays (Hobbs et al. 2010).
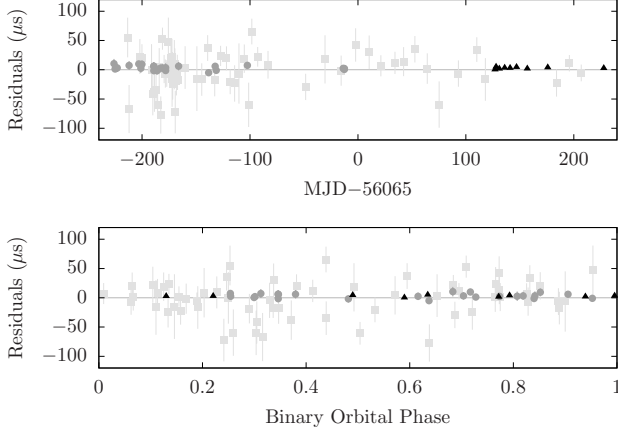
3. TIMING RESULTS

Figure 2. The TOA residuals of our timing model as a function of MJD (upper panel) and binary orbital phase (lower panel). Light-grey squares show TOA residuals from observations with the 76-m Lovell telescope, dark-gray circles residuals from observations with the Arecibo telescope using the ALFA receiver and the Mock spectrometers, and black triangles observations with the Arecibo telescope using the L-wide receiver and the PUPPI backend. The TOA residual distribution does not exhibit any clear trends.

Astrometric, spin, and binary parameters, including the relativistic periastron advance, were determined from the timing analysis of the TOAs described in the previous section. Table 1 shows the parameters of our timing solution obtained with TEMPO2.

The pulsar's mass function is given by

$$f_1 = \frac{4\pi^2 x_1^3}{T_\odot P_{\rm orb}^2} = \frac{M_2^3 \sin^3(i)}{(M_1 + M_2)^2}, \qquad (2)$$

where $x_1 = a_1 \sin(i)/c$ is the pulsar's projected orbital semi-major axis in light-seconds, $T_\odot = GM_\odot/c^3 = 4.925490947\,\mu$s is the solar mass in time units, $P_{\rm orb}$ is the orbital period, and M_1 and M_2 are the masses of the pulsar and the companion in units of solar masses, respectively. We find $f_1 = 0.00626918(2)\,M_\odot$, which indicates a low-mass companion with a minimum mass $M_2 \geq 0.253\,M_\odot$, which is obtained for $i = 90°$ and a pulsar mass $M_1 = 1.35\,M_\odot$. The median companion mass, assuming $i = 60°$, is $M_{2,\rm med} = 0.297\,M_\odot$. Therefore, the binary companion is most likely a helium WD.

Considering the system's mass function, its high spin frequency $\nu = 232.300$ Hz and small spin period derivative, PSR J1950+2414 is very similar to the majority of comparable binary pulsar systems in the Galactic field. The most probable nature for the system would therefore be a fully recycled millisecond pulsar with a WD companion. In this case, mass transfer from the WD progenitor to the MSP in the system's past would have circularized the binary orbit, spun up the pulsar, and damped its magnetic field, as described in Section 1.

However, the orbital eccentricity $e = 0.07981158(12)$ of PSR J1950+2414 is larger (by roughly two orders of magnitude or more) than that of all millisecond pulsars with helium WD companions in the Galactic field with the exception of the three recently discovered similar systems (see Sections 1 and 4).

The theory of general relativity predicts an advance of the longitude of periastron, depending on the total mass of the system, its eccentricity and orbital period (Weisberg & Taylor

Parameter	Value[a]
General Information	
MJD Range	55839.0—56292.7
Number of TOAs	94
Weighted RMS of Timing Residuals (μs)	4.7
Reduced-χ^2 value	1.2
MJD of Period Determination	55839
Binary Model Used	BT
Fitted Parameters	
R.A., α (J2000)	19:50:45.06390(10)
Dec., δ (J2000)	+24:14:56.9638(11)
MJD of Position Determination	55839
Spin Frequency, ν (Hz)	232.30014862462(14)
Spin Frequency Derivative, $\dot{\nu}$ ($\times 10^{-15}$ Hz s^{-1})	$-1.020(6)$
Dispersion Measure, DM (pc cm^{-3})	142.089(18)[b]
MJD of DM Determination	55839
Projected Semi-Major Axis, $a_1 \sin(i)$ (lt-s)	14.2199738(11)
Orbital Period, $P_{\rm orb}$ (days)	22.1913727(10)
Epoch of periastron, T_0 (MJD)	55846.0226219(15)
Longitude of periastron, ω_0 (deg)	274.4155(3)
Periastron advance, $\dot{\omega}$ (deg yr^{-1})	0.0020(3)
Orbital eccentricity, e	0.07981158(12)
Derived Parameters	
Spin Period, P (ms)	4.304775549739(2)
Spin Period Derivative, $\dot{P}$ ($\times 10^{-20}$)	1.8900(10)
Intrinsic $\dot{P}$, $\dot{P}_{\rm int}$ ($\times 10^{-20}$)	$\leq 2.1166(10)$[c]
Galactic longitude, l (deg)	61.10
Galactic latitude, b (deg)	-1.17
Distance, d (NE2001, kpc)	$5.5^{+0.8}_{-0.8}$
Mass Function, f_1 ($M_\odot$)	0.00626918(2)
Minimum companion mass M_2 ($M_\odot$)	0.253
Total Mass, M ($M_\odot$)	2.3(4)
Characteristic Age, $\tau_c = P/(2\dot{P})$ (Gyr)	≥ 3.2[c]
Surface Magnetic Field Strength, $B_{\rm S}$ ($\times 10^8$ G)	≤ 3.1[c]
Spin-down Luminosity, $\dot{E}$ ($\times 10^{34}$ ergs/s)	≤ 1.0[c]

[a] The numbers in parentheses are the 1-σ, TEMPO2-reported uncertainties on the last digit(s). Uncertainties in the pulsar distance inferred from NE2001 are assuming a 20% uncertainty in DM to account for model uncertainties.
[b] The solution here is based on single-frequency TOAs per Arecibo and Jodrell Bank observations, respectively. Fitting the DM is therefore degenerate with fitting the JUMPs between the data sets. The DM and its uncertainty were therefore fitted from TOAs obtained in two sub-bands for the Arecibo data combined with the Jodrell Bank TOAs, and kept fixed for the solution presented here.
[c] The observed period derivative has been corrected for Galactic acceleration. We cannot correct for the Shklovskii effect, and therefore the value of $\dot{P}_{\rm int}$ is an upper limit, see Section 3. Its reported uncertainty here does not include the uncertainty from the Galactic model. τ_c, $B_{\rm S}$, and $\dot{E}$ have been inferred from $\dot{P}_{\rm int}$.

1981), given by

$$\dot{\omega} = 3 \left(\frac{P_{\rm orb}}{2\pi}\right)^{-5/3} \frac{(T_\odot (M_1 + M_2))^{2/3}}{1 - e^2}, \qquad (3)$$

where $P_{\rm orb}$, M_1, M_2 and $T_\odot$ are defined as above and e is the orbital eccentricity.

Our observations of PSR J1950+2414 significantly detect the system's periastron advance $\dot{\omega} = 0.0020(3)$ deg yr^{-1}. This corresponds to an inferred total mass of $M = M_1 + M_2 = 2.3(4)\,M_\odot$, where the uncertainty is dominated by the uncertainty in $\dot{\omega}$. This measurement is suggestive of a NS significantly more massive than $1.35\,M_\odot$, however, it is currently not precise enough to infer the individual masses of the pulsar and/or the companion star. We expect our ongoing observation campaign to significantly improve the measurement of $\dot{\omega}$ and therefore the estimate of the total mass.

Ongoing timing observations might also help to constrain or measure the Shapiro delay in the binary system. Combined measurements of the Shapiro delay and the periastron advance

can be used to infer the separate masses of both components (Freire & Wex 2010).

The observed spin period derivative $\dot{P}$ has been corrected for Galactic acceleration (Nice & Taylor 1995), to obtain a value of the spin period derivative of $\dot{P}_{corr} = 2.12 \times 10^{-20}$. This takes into account a Galactic acceleration model that uses the radial velocity curve published in Reid et al. (2014). However, since the proper motion currently cannot be measured with useful accuracy, we cannot correct for the contribution $\dot{P}_{Shk}$ to the period derivative from the Shklovskii effect (Shklovskii 1970), and therefore we can only estimate an upper limit for the intrinsic $\dot{P}_{int}$.

Both the intrinsic $\dot{P}_{int}$ and the Shklovskii effect contribution $\dot{P}_{Shk}$ are always positive and fulfill $\dot{P}_{int} + \dot{P}_{Shk} = \dot{P}_{corr}$. Therefore, assuming $\dot{P}_{Shk} = 0$, we obtain an upper limit to the intrinsic spin period derviative of $\dot{P}_{int} \leq 2.12 \times 10^{-20}$. On the other hand, assuming $\dot{P}_{int} = 0$ we can constrain the total proper motion to ≤ 19 mas/yr.

From $\dot{P}_{int} = 2.12 \times 10^{-20}$ s s^{-1} we infer a lower limit for the characteristic age of $\tau_c \geq 3.2$ Gyr and upper limits for the the surface magnetic field strength $B_S \leq 3.1 \times 10^8$ G and spin-down luminosity $\dot{E} \leq 1.0 \times 10^{34}$ ergs/s. These parameters are very similar to those of the general MSP population.

3.1. *Counterparts at other Wavelengths*

Let us now consider whether PSR J1950+2414 is observable at X-ray and γ-ray wavelengths and whether the nature of its companion can be established by way of optical/IR observations.

The field around PSR J1950+2414 has not been previously targeted in a pointed observation by any former or current X-ray mission. A 581-s exposure from the *ROSAT* all-sky survey is too shallow to yield any useful constrains on the X-ray flux from the pulsar. Based on its $\dot{E}$, PSR J1950+2414 likely has a soft, thermal X-ray spectrum due to heating of its magnetic polar caps, with $L_X \approx 10^{-4} - 10^{-3}\dot{E} \sim 10^{30-31}$ erg s^{-1}, as typically seen in non-eclipsing MSPs (Zavlin 2006; Bogdanov et al. 2006). At a distance of 5.5 kpc and assuming an absorbing column of $N_H \approx 4 \times 10^{21}$ cm^{-2} (based on the empirical DM-N_H relation from He et al. 2013) a detection of the pulsar with *Chandra* or *XMM-Newton* would require impractically long exposures.

There is no *Fermi* LAT Third Point Source Catalog (3FGL; The Fermi-LAT Collaboration 2015) object in the vicinity of PSR J1950+2414's position. A visual inspection of the *Fermi* LAT data from the beginning of the mission up to 2015 January 19 shows no excess emission at the pulsar position. This is expected given that at the Galactic latitude of PSR J1950+2414 ($b = -1.1°$), the diffuse γ-ray background is overwhelming. In addition, the commonly used γ-ray "detectability" metric for pulsars, $\sqrt{\dot{E}}/D^2$ is 3×10^{15} erg$^{1/2}$ s$^{-1/2}$ kpc^{-2} for PSR J1950+2414, substantially lower compared to MSPs detected by *Fermi* LAT (see, e.g., Figure 15 in Abdo et al. 2013) so it is not expected to be a bright γ-ray source.

In principle, the nature of the companion of PSR J1950+2414 can be established by way of optical/IR observations. If the secondary is a main sequence star – in this case PSR J1950+2414 would belong to the same class as of systems as PSR J1903+0327 – it is likely to be a M3.5 red dwarf based on the mass measurement from radio timing (~ 0.25 M$_\odot$). Data from the Digitized Sky Survey reveal no optical counterpart at the radio position of the MSP, likely because it is too distant and extincted. Indeed, using the relations by Predehl & Schmitt (1995) and He et al. (2013)

combined with the pulsar's dispersion measure, we estimate the visual extinction to the target to be $A_V \approx 2.3$. Taking the absolute magnitude of a M3.5V star, $M_V \approx 11.5$ (Henry et al. 2002), and scaling with the dispersion measure derived distance (≈ 5.5 kpc) yields an expected apparent magnitude of $V \approx 27.5$ including extinction.

If we consider the intrinsic colors of an M3.5V star based on 2MASS data (Lépine & Gaidos 2011), and scale the extinction with wavelength (based on Cardelli et al. 1989), we obtain apparent magnitudes in the near-IR of $J \approx 23.9$, $H \approx 23.1$ and, $K \approx 22.6$. Based on this, it is evident that near-IR imaging observations provide the better means of establishing the nature of the companion, which in turn helps constrain the evolutionary history of PSR J1950+2414. Existing near-IR data from the 2MASS all-sky survey (Skrutskie et al. 2006) show no counterpart at the pulsar position, although this provides no meaningful constraints on the PSR J1950+2414 companion since the limiting magnitude is only ~ 16. Thus, deeper near-IR observations are required.

If the companion star is a He WD, its absolute magnitude is $15 > M_V > 10$ (Kaler 2006). The extinction given above and the DM-inferred pulsar distance yield an apparent magnitude of $31 \gtrsim m_V \gtrsim 26$. Detection in the visual band in imaging observations with 8-meter class telescopes requires apparent magnitudes of $m_V < 24$ (Bates et al. 2015). Therefore, a detection or spectroscopic identification of an He WD companion in the optical band is currently impossible.

4. DISCUSSION

PSR J1950+2414 has an unusual combination of small pulsar spin period and high orbital eccentricity. The small spin period and small spin period derivative (and inferred surface magnetic field) point to a long recycling episode in the system's past, in which matter from the companion star accreted onto the pulsar, spun it up and reduced its magnetic field. Yet, the high orbital eccentricity appears at odds with this picture because long recycling episodes are believed to circularize the binary orbits to eccentricities in the range $e = 10^{-7} - 10^{-3}$ (Phinney 1992).

Thus, these systems must form through different channels and/or experience some mechanism that increases the orbital eccentricity after the pulsar is recycled. We will discuss four proposed channels: 1) Formation in a hierarchical triple system which became unstable and ejected one of its members; 2) Perturbations in regions with high stellar density (globular clusters); 3) The rotationally delayed accretion-induced collapse of a super-Chandrasekhar white dwarf; 4) Dynamical interaction of the binary with a circumbinary disk.

Table 2 compares our discovery with the four known eccentric MSPs in the Galactic field.

The similarity of the spin and orbital parameters of PSR J1950+2414 to those of PSR J2234+06 and PSR J1946+3417 (and also, to a lesser extent, to PSR J1618−3921) is striking, and is further evidence for the existence of a common formation mechanism that is clearly distinct from that of PSR J1903+0327 (which, as mentioned before, likely resulted from the chaotic disruption of a triple system, as indicated by its more massive main-sequence companion, much larger eccentricity and orbital period). PSR J1618−3921 differs from the aforementioned pulsars by a longer spin period and less eccentric orbit, however the orbital period is similar to that of PSR J1950+2414, supporting the idea that something anomalous happens within this range of orbital periods.

Table 2
Physical parameters of the five known eccentric MSPs. PSR J1903+0327 (Champion et al. 2008) was most likely formed from a triple system. PSR J1618−3921 (data reproduced from Edwards & Bailes 2001, Bailes 2010, and Bailes – private communication), two recently discovered MSPs (data from Freire & Tauris 2014; Barr et al. 2013; Deneva et al. 2013) and PSR J1950+2414 (from this publication) have very similar orbital and spin characteristics, suggesting a common formation channel. The height above the Galactic plane, z, was calculated from the DM-inferred distance and the Galactic latitude.

Pulsar	P	$P_{\rm orb}$	$M_{2,\rm med}$	e	$|z|$
PSR J1903+0327	2.1 ms	95.2 days	$1.1\,M_\odot$	0.44	0.1 kpc
PSR J2234+06	3.6 ms	32 days	$0.23\,M_\odot$	0.13	0.4 kpc
PSR J1946+3417	3.2 ms	27 days	$0.24\,M_\odot$	0.14	0.5 kpc
PSR J1618−3921	12.0 ms	22.8 days	$0.20\,M_\odot$	0.027	0.6 kpc
PSR J1950+2414	**4.3 ms**	**22.2 days**	**$0.30\,M_\odot$**	**0.08**	**0.1 kpc**

All pulsars in Table 2 have small distances from the Galactic plane $|z| \lesssim 0.6\,{\rm kpc}$. If the systems were produced by 2) exchange interactions in globular clusters, their distances to the Galactic plane are expected to be large, similar to the values for the globular cluster population (Harris 1996). Therefore, it is unlikely that any of the pulsars originated in a globular cluster. Future observations of PSR J1950+2414 might be used to constrain its proper motion and further elucidate the issue.

As described in Section 1, Freire & Tauris (2014) recently have proposed the formation mechanism 3) for fully recycled MSPs in eccentric orbits. Since PSR J1950+2414 is such a system, let us now consider whether it could have also formed by the same mechanism.

At the center of their model is an accretion-induced collapse of a super-Chandrasekhar mass white dwarf in a close binary. The WD only collapses after the end of the accretion episode, and after it has lost sufficient spin angular momentum, directly producing an MSP in an eccentric orbit. Based on their simulations, Freire & Tauris (2014) provide a list of predictions for MSP systems formed through the rotationally delayed AIC channel. At the current time, PSR J1950+2414 is consistent with these predictions as detailed in the following.

From Fig. 3 in Freire & Tauris (2014), and assuming a range of pre-AIC WD masses between 1.37 and $1.48\,M_\odot$, isotropically directed kicks, and initial orbital periods between 15 and 30 days, the kick velocity must be around $2\,{\rm km\,s}^{-1}$ to yield orbital eccentricities between 0.09 and 0.14. The orbital eccentricity of PSR J1950+2414 is just outside the lower end of that range (and that certainly is the case for PSR J1618−3921). This might suggest a slightly larger kick magnitude and a slightly wider range of eccentricities to be observed in these systems in the future, or a slightly smaller NS binding energy than that assumed in that simulation.

The companion should be a He WD with a mass in the range $0.24 - 0.31\,M_\odot$, as predicted by the $P_{\rm orb}$-$M_{\rm WD}$ relation from Fig. 5 in Tauris & Savonije (1999) for this orbital period of 22 days. Although we cannot currently determine the nature of the companion of PSR J1950+2414, its median companion mass of $0.30\,M_\odot$ is certainly compatible with this expectation.

Freire & Tauris (2014) predict a pulsar mass of typically $1.22 - 1.31\,M_\odot$. Currently, we have not measured the total mass of the system to a sufficiently high precision to test this prediction.

The system has low Galactic height, as expected from systems that formed with very small kick velocity ($\lesssim 10\,{\rm km/s}$) in an AIC event. Indeed, the low Galactic heights of the MSPs

in eccentric orbits discovered to date suggests small peculiar space velocities compared to the general MSP population. This assumption might be further tested with a future measurement of the proper motion of the system.

The characteristics of PSR J1950+2414 are also consistent with dynamical interaction with a circumbinary disk (Antoniadis 2014). The circumbinary disk model makes two predictions which could be tested for PSR J1950+2414 with further observations: 1) As in Freire & Tauris (2014), the companions should also be He WDs with masses given by Tauris & Savonije (1999), which as we have seen agrees with our current mass constraint for the companion of PSR J1950+2414. 2) The masses of the MSP and the peculiar space velocities should closely resemble those of circular binary MSPs, unlike the *small* velocities ($\lesssim 10\,{\rm km/s}$) predicted by the AIC model. With our current timing data, we cannot constrain the proper motion and can therefore neither confirm nor falsify this prediction.

Whatever the formation scenario for systems like PSR J1950+2414 is, it has in this case produced an object with an inferred surface magnetic field comparable to the general MSP population. This does not falsify any of the models discussed above, but might be useful constraint on other possible formation scenarios.

The fact that the characteristic age ($\tau_c \geq 3.2\,{\rm Gyr}$) is very similar to that of the general MSP population can be used to formulate a first rough estimate of the occurrence of these systems. It suggests that the relative frequency of occurrence of PSR J1950+2414-like MSPs in the population is comparable to the fraction of the currently known systems in the currently known population. Assuming that PSRs J1618−3921, J1946+3417, J1950+2414, and J2234+06 all formed through the same mechanism and all have similar τ_c, the relative frequency of these systems is of order 4 of a total of 230 known MSPs[30] not associated with a globular cluster, roughly 2% of the population.

5. CONCLUSIONS AND FUTURE WORK

We have presented the discovery and initial timing of the fully-recycled ($P = 4.3\,{\rm ms}$) MSP PSR J1950+2414 in an eccentric ($e = 0.08$) orbit ($P_{\rm orb} = 22\,{\rm days}$) with a median companion mass of $0.3\,M_\odot$. PSR J1950+2414 is only the fifth system with a large eccentricity to be discovered. Its spin and orbital parameters are similar to those of three previously known systems with orbital periods in the range of $\sim 20 - 30$ days, spin periods between 2 ms and 12 ms, large orbital eccentricities ($0.03 \lesssim e \lesssim 0.15$), and companions with masses $0.2\,M_\odot \lesssim m_{\rm c} \lesssim 0.3\,M_\odot$.

This combination of parameters cannot be explained in the standard pulsar recycling scenario. The existence of now four known similar systems which probably have a helium WD companion suggests the existence of a common formation channel leading to these unusual MSP systems. The upper limit on the intrinsic spin period and the inferred surface magnetic field are comparable to those of the general MSP population.

We compared the properties of PSR J1950+2414 with the predictions of four proposed formation channels. The initial evolution of the pulsar in a hierarchical triple and the origin in an exchange encounter in an high stellar density environment (e.g., globular cluster) are unlikely. Although we cannot conclusively rule out or confirm formation through a rotationally-

[30] http://astro.phys.wvu.edu/GalacticMSPs/GalacticMSPs.txt

delayed AIC event or interaction with a circumbinary disk with the measurements presented here, future observations might allow us to test a variety of predictions made by the different possible formation models.

The pulsar is currently being observed with Arecibo Observatory, and this will allow us to better constrain the pulsar and companion masses, which is of highest importance to discriminate between the AIC model and the circumbinary-disk model. The individual masses of the pulsar and the companion can be obtained from combining observations of the relativistic periastron advance with observations of the Shapiro delay. Using the orthometric parametrization of the Shapiro delay from Freire & Wex (2010) should provide the most precise estimates of the individual masses. The uncertainties of the periastron advance and the Shapiro delay in this parametrization are less degenerate than in the standard parametrization. Therefore, even if the measurement of the Shapiro delay has larger errors, a precise measurement of the relativistic periastron advance will allow for well-defined pulsar mass determination, see, e.g., Lynch et al. (2012). The ongoing observations will improve the relativistic periastron advance measurement and might also lead to a detection of the Shapiro delay.

Radio observations with longer time baselines will provide upper limits on or a measurement of the proper motion of the pulsar, and therefore of its peculiar space velocity. The AIC model predicts small values ($\lesssim 10$ km/s), while the circumbinary-disk model predicts larger values. Measuring the proper motion could therefore permit discrimination between the two models.

Further information about the nature of the companion might be obtained from observations at optical or infrared wavelengths, as detailed in Section 3.1. Near-IR imaging observations provide the best means of establishing the nature of the companion, which in turn helps constrain the evolutionary history of PSR J1950+2414.

Modern pulsar surveys like PALFA are probing the Galactic disk to unprecedented depths and are likely to find other such systems. Having a larger sample size will allow discriminating between the different proposed models with greater confidence than is possible now.

---

[31] Where the real name is unknown or must remain confidential we give the *Einstein@Home* user name and display it in single quotes.

REFERENCES

Aasi, J., Abadie, J., Abbott, B. P., et al. 2013, Phys. Rev. D, 87, 042001

Abbott, B., Abbott, R., Adhikari, R., et al. 2009a, Phys. Rev. D, 79, 022001

Abbott, B. P., Abbott, R., Adhikari, R., et al. 2009b, Phys. Rev. D, 80, 042003

Abdo, A. A., Ajello, M., Allafort, A., et al. 2013, ApJS, 208, 17

Allen, B., Knispel, B., Cordes, J. M., et al. 2013, ApJ, 773, 91

Alpar, M. A., Cheng, A. F., Ruderman, M. A., & Shaham, J. 1982, Nature, 300, 728

Anderson, D. P., Christensen, C., & Allen, B. 2006, in Proceedings of the 2006 ACM/IEEE conference on Supercomputing, SC '06 (New York, NY, USA: ACM)

Antoniadis, J. 2014, ApJ, 797, L24

Antoniadis, J., Freire, P. C. C., Wex, N., et al. 2013, Science, 340, 448

Archibald, A. M., Stairs, I. H., Ransom, S. M., et al. 2009, Science, 324, 1411

Archibald, A. M., Bogdanov, S., Patruno, A., et al. 2014, ArXiv e-prints, arXiv:1412.1306 [astro-ph.HE]

Aulbert, C., & Fehrmann, H. 2009, Max-Planck-Gesellschaft Jahrbuch 2009

Backer, D. C., Kulkarni, S. R., Heiles, C., Davis, M. M., & Goss, W. M. 1982, Nature, 300, 615

Bailes, M. 2010, New Astronomy Reviews, 54, 80

Barr, E. D., Champion, D. J., Kramer, M., et al. 2013, MNRAS, 435, 2234

Bassa, C. G., Patruno, A., Hessels, J. W. T., et al. 2014, MNRAS, 441, 1825

Bates, S. D., Thornton, D., Bailes, M., et al. 2015, MNRAS, 446, 4019

Bildsten, L., Chakrabarty, D., Chiu, J., et al. 1997, ApJS, 113, 367

Blandford, R., & Teukolsky, S. A. 1976, ApJ, 205, 580

Bogdanov, S., Grindlay, J. E., Heinke, C. O., et al. 2006, ApJ, 646, 1104

Cardelli, J. A., Clayton, G. C., & Mathis, J. S. 1989, ApJ, 345, 245

Champion, D. J., Ransom, S. M., Lazarus, P., et al. 2008, Science, 320, 1309

Chen, H.-L., Chen, X., Tauris, T. M., & Han, Z. 2013, ApJ, 775, 27

Cordes, J. M., Freire, P. C. C., Lorimer, D. R., et al. 2006, ApJ, 637, 446

Crawford, F., Stovall, K., Lyne, A. G., et al. 2012, ApJ, 757, 90

Demorest, P. B., Pennucci, T., Ransom, S. M., Roberts, M. S. E., & Hessels, J. W. T. 2010, Nature, 467, 1081

Deneva, J. S., Stovall, K., McLaughlin, M. A., et al. 2013, ApJ, 775, 51

Deneva, J. S., Freire, P. C. C., Cordes, J. M., et al. 2012, ApJ, 757, 89

Edwards, R. T., & Bailes, M. 2001, ApJ, 553, 801

Edwards, R. T., Hobbs, G. B., & Manchester, R. N. 2006, MNRAS, 372, 1549

Freire, P. C. C., & Tauris, T. M. 2014, MNRAS, 438, L86

Freire, P. C. C., & Wex, N. 2010, MNRAS, 409, 199

Freire, P. C. C., Bassa, C. G., Wex, N., et al. 2011, MNRAS, 412, 2763

Harris, W. E. 1996, AJ, 112, 1487

He, C., Ng, C.-Y., & Kaspi, V. M. 2013, ApJ, 768, 64

Heggie, D. C., & Rasio, F. A. 1996, MNRAS, 282, 1064

Henry, T. J., Walkowicz, L. M., Barto, T. C., & Golimowski, D. A. 2002, AJ, 123, 2002

Hessels, J. W. T., Ransom, S. M., Stairs, I. H., et al. 2006, Science, 311, 1901

Hobbs, G., Archibald, A., Arzoumanian, Z., et al. 2010, Classical and Quantum Gravity, 27, 084013

Hobbs, G. B., Edwards, R. T., & Manchester, R. N. 2006, MNRAS, 369, 655

Hotan, A. W., van Straten, W., & Manchester, R. N. 2004, Publications of the Astronomical Society of Australia, 21, 302

Kaler, J. B. 2006, The Cambridge Encyclopedia of Stars

Knispel, B. 2011, PhD thesis, Leibniz Universität Hannover

Knispel, B., Allen, B., Cordes, J. M., et al. 2010, Science, 329, 1305

Knispel, B., Lazarus, P., Allen, B., et al. 2011, ApJ, 732, L1

Knispel, B., Eatough, R. P., Kim, H., et al. 2013, ApJ, 774, 93

Lazarus, P., Tauris, T. M., Knispel, B., et al. 2014, MNRAS, 437, 1485

Lépine, S., & Gaidos, E. 2011, AJ, 142, 138

Lorimer, D. R., & Kramer, M. 2012, Handbook of Pulsar Astronomy

Lynch, R. S., Freire, P. C. C., Ransom, S. M., & Jacoby, B. A. 2012, ApJ, 745, 109

Manchester, R. N., Hobbs, G. B., Teoh, A., & Hobbs, M. 2005, AJ, 129, 1993

Nice, D. J., & Taylor, J. H. 1995, ApJ, 441, 429

Papitto, A., Ferrigno, C., Bozzo, E., et al. 2013, Nature, 501, 517

Patruno, A., Archibald, A. M., Hessels, J. W. T., et al. 2014, ApJ, 781, L3

Phinney, E. S. 1992, Royal Society of London Philosophical Transactions Series A, 341, 39

Phinney, E. S., & Kulkarni, S. R. 1994, ARA&A, 32, 591

Pijloo, J. T., Caputo, D. P., & Portegies Zwart, S. F. 2012, MNRAS, 424, 2914

Pletsch, H. J. 2010, Phys. Rev. D, 82, 042002

—. 2011, Phys. Rev. D, 83, 122003

Pletsch, H. J., & Allen, B. 2009, Physical Review Letters, 103, 181102

Pletsch, H. J., Guillemot, L., Allen, B., et al. 2012, ApJ, 744, 105

—. 2013, ApJ, 779, L11

Portegies Zwart, S., van den Heuvel, E. P. J., van Leeuwen, J., & Nelemans, G. 2011, ApJ, 734, 55

Predehl, P., & Schmitt, J. H. M. M. 1995, A&A, 293, 889

Radhakrishnan, V., & Srinivasan, G. 1982, Current Science, 51, 1096

Ransom, S. M., Hessels, J. W. T., Stairs, I. H., et al. 2005, Science, 307, 892

Ransom, S. M., Stairs, I. H., Archibald, A. M., et al. 2014, Nature, 505, 520

Rasio, F. A., & Heggie, D. C. 1995, ApJ, 445, L133

Reid, M. J., Menten, K. M., Brunthaler, A., et al. 2014, ApJ, 783, 130

Roberts, M. S. E. 2013, in IAU Symposium, Vol. 291, IAU Symposium, ed. J. van Leeuwen, 127

Roy, J., Ray, P. S., Bhattacharyya, B., et al. 2015, ApJ, 800, L12

Shklovskii, I. S. 1970, Soviet Ast., 13, 562

Skrutskie, M. F., Cutri, R. M., Stiening, R., et al. 2006, AJ, 131, 1163

Smarr, L. L., & Blandford, R. 1976, ApJ, 207, 574

Stairs, I. H. 2004, Science, 304, 547

Stappers, B. W., Archibald, A. M., Hessels, J. W. T., et al. 2014, ApJ, 790, 39

Swiggum, J. K., Lorimer, D. R., McLaughlin, M. A., et al. 2014, ApJ, 787, 137

Tauris, T. M., & Savonije, G. J. 1999, A&A, 350, 928

Tauris, T. M., & van den Heuvel, E. P. J. 2014, ApJ, 781, L13

The Fermi-LAT Collaboration. 2015, ArXiv e-prints, arXiv:1501.02003 [astro-ph.HE]

Weisberg, J. M., & Taylor, J. H. 1981, General Relativity and Gravitation, 13, 1

Wijnands, R., & van der Klis, M. 1998, Nature, 394, 344

Zavlin, V. E. 2006, ApJ, 638, 951

Zhu, W. W., Berndsen, A., Madsen, E. C., et al. 2014, ApJ, 781, 117